Journal of the Mechanics and Physics of Solids 56 (2008) 3475–3485

Contents lists available at ScienceDirect

Journal of the Mechanics and Physics of Solids

journal homepage: www.elsevier.com/locate/jmps

Nonlocal shell model for elastic wave propagation in single- and double-walled carbon nanotubes

Yan-Gao Hu [a], K.M. Liew [a,*], Q. Wang [b], X.Q. He [a], B.I. Yakobson [c]

[a] Department of Building and Construction, City University of Hong Kong, Hong Kong
[b] Department of Mechanical and Manufacturing Engineering, University of Manitoba, Winnipeg, Manitoba, Canada R3T 5V6
[c] ME&MS Department, Rice University, MS 321, Houston, TX 77005-1892, USA

ARTICLE INFO

Article history:
Received 28 February 2008
Received in revised form
11 July 2008
Accepted 19 August 2008

Keywords:
Carbon nanotube
Elastic wave
Molecular dynamics
Nonlocal shell model
Small-scale effect

ABSTRACT

This paper investigates the transverse and torsional wave in single- and double-walled carbon nanotubes (SWCNTs and DWCNTs), focusing on the effect of carbon nanotube microstructure on wave dispersion. The SWCNTs and DWCNTs are modeled as nonlocal single and double elastic cylindrical shells. Molecular dynamics (MD) simulations indicate that the wave dispersion predicted by the nonlocal elastic cylindrical shell theory shows good agreement with that of the MD simulations in a wide frequency range up to the terahertz region. The nonlocal elastic shell theory provides a better prediction of the dispersion relationships than the classical shell theory when the wavenumber is large enough for the carbon nanotube microstructure to have a significant influence on the wave dispersion. The nonlocal shell models are required when the wavelengths are approximately less than 2.36×10^{-9} and 0.95×10^{-9} m for transverse wave in armchair (15,15) SWCNT and torsional wave in armchair (10,10) SWCNT, respectively. Moreover, an MD-based estimation of the scale coefficient e_0 for the nonlocal elastic cylindrical shell model is suggested. Due to the small-scale effects of SWCNTs and the interlayer van der Waals interaction of DWCNTs, the phase difference of the transverse wave in the inner and outer tube can be observed in MD simulations in wave propagation at high frequency. However, the van der Waals interaction has little effect on the phase difference of transverse wave.

1. Introduction

Carbon nanotubes (CNTs) have attracted worldwide attention (Iijima, 1991; Ball, 2001; Baughman et al., 2002) for their wide range of applications, including atomic force microscopes, field emitters, frictionless nano-actuators, nano-motors, nano-bearings, nano-springs, nano-fillers for composite materials, and nano-scale electronic devices (Lau, 2003). In addition to experimental endeavors, CNT modeling is classified into two main categories. The first is atomic modeling, which includes such techniques as classical molecular dynamics (MD) and tight-binding MD and the density functional model (Iijima et al., 1996; Hernandez et al., 1998; Sanchez-Portal et al., 1999; Yakobson et al., 1997; Liew et al., 2004b). Li and Chou (2006) reported an atomistic simulation of single-walled CNTs (SWCNTs) subjected to harmonic waves. Atomic modeling is limited to systems with a small number of molecules and atoms and is therefore confined to small-scale modeling. The second category is continuum modeling (Yakobson et al., 1996; Krishnan et al., 1998; Ru, 2000a, b;

* Corresponding author.
E-mail address: kmliew@cityu.edu.hk (K.M. Liew).

0022-5096/$ - see front matter © 2008 Elsevier Ltd. All rights reserved.
doi:10.1016/j.jmps.2008.08.010

Parnes and Chiskis, 2002), which includes classical (or local) beam and shell theories that are practical for analyzing CNTs for large-scale systems. Successful work has been conducted with continuum modeling, such as buckling analysis, dynamics studies, and mechanical property investigations of CNTs (Wong et al., 1997; Lourie et al., 1998; Govindjee and Sackman, 1999; Wang et al., 2005; Natsuki et al., 2006; Liew et al., 2004a, 2006; Liew and Wang, 2007). Natsuki et al. (2007) investigated the wave propagation in SWCNTs and double-walled carbon nanotubes (DWCNTs) conveying fluid through the use of the shell model. Insepov et al. (2006) summarized a few ways to activate surface-traveling waves on the nanotube surface.

Although the classical continuum models are efficient in CNT mechanical analysis through their relatively simple formulae, their applicability to the identification of the small-scale effect on the mechanical behavior of CNTs is questionable. This limited applicability of the classical or local continuum models at small-length scales is partly due to the fact that classical modeling does not admit intrinsic size dependence in the elastic solutions of inclusions and inhomogeneities. Sun and Zhang (2003) discussed the limited applicability of continuum models to nanotechnology and proposed a semi-continuum model to analyze nano-materials. The values of the material properties were found to be completely dependent on the thickness of the plate structure. The modeling of such a size-dependent phenomenon has become an active and interesting subject of research in continuum modeling (Sheehan and Lieber, 1996; Yakobson et al., 1997). Wang (2004) demonstrated the effective in-plane stiffness and bending rigidity of armchair and zigzag CNTs through analysis of the representative volume element of a graphene layer with continuous elastic models. It was found that the bending rigidity of the CNTs had a size effect. Wang and Hu (2005) studied flexural wave propagation in SWCNT through the use of a nonlocal elastic Timoshenko beam model and an MD simulation based on the first-generation reactive empirical bond order (REBO) potential (Brenner, 1990). Liew et al. (2008) studied the flexural wave propagation in SWCNT through the use of an MD simulation based on the second-generation REBO (Brenner et al., 2002). The material microstructure at small size, such as the lattice spacing between individual atoms, becomes increasingly important and the discrete structure of the material can no longer be homogenized into a continuum. Therefore, the nonlocal elastic continuum model is expected to take into account the scale effect when tackling large-scale nano-material analysis. Size effects often become prominent at nanometer scales, and there is increasing interest in the general area of nanotechnology in explicitly addressing the cause of these effects (Sharma et al., 2003).

The nonlocal elasticity theory (Eringen, 1976, 1983) assumes that the stress state at a given reference point is a function of the strain field at every point in the body. Therefore, the scale effect can be considered in constitutive equations simply as a material parameter. However, the classical elasticity theory cannot account for the scale effect, as the stress state is uniquely dependent on the strain state at the same point. Peddieson et al. (2003) expected the application of the nonlocal elasticity theory to have potential in the analysis of nano-materials. They applied it to the formulation of a nonlocal version of the Euler–Bernoulli beam model and concluded that nonlocal continuum mechanics could potentially play a useful role in nanotechnology applications. Further applications of nonlocal continuum mechanics have been employed in the study of CNT buckling. Sudak (2003) presented a multiple-column model for the linearized column buckling of multi-walled CNTs using the theory of nonlocal continuum mechanics. Zhang et al. (2004) proposed a nonlocal multi-shell model for the axial buckling of multi-walled nanotubes (MWNTs) under axial compression. The nonlocal elastic Euler–Bernoulli and Timoshenko beam models were applied to study wave propagation in CNTs (Wang, 2005). Wang and Varadan (2007) studied wave propagation in CNTs based on the nonlocal elastic shell theory. Both theoretical analyses and numerical simulations have explicitly revealed the small-scale effect on wave dispersion relations for different CNT wavenumbers in the longitudinal and circumferential directions and for different wavelengths in the circumferential direction. However, no MD simulations have been available for the validation of shell models in studying transverse and torsional wave propagation in CNTs.

This paper aims to use nonlocal shell models to study transverse and torsional wave in SWCNTs and DWCNTs and to provide verification of these models by using MD simulation. The paper is organized as follows. In Section 2, the nonlocal elastic shell theory is applied to model SWCNTs and DWCNTs. The dispersion of the transverse waves is calculated. An estimation of the scale coefficient is also provided. In Section 3, the MD model based on the second-generation REBO potential is outlined. Section 4 presents a discussion of the MD results, and concluding remarks are included in Section 5.

2. Nonlocal elastic shell theory

In nonlocal elasticity (Eringen, 1976), the stress at a reference point x is considered to be a function of the strain field at every point in the body. The basic equations for linear, homogeneous, isotropic, and nonlocal elastic solids with zero body force are given as follows (Eringen, 1983):

$$\sigma_{ij,j} = 0, \tag{1a}$$

$$\sigma_{ij}(x) = \int \alpha(|x - x'|, \tau) C_{ijkl} \varepsilon_{kl}(x') \, \mathrm{d}V(x'), \quad \forall x \in V, \tag{1b}$$

$$\varepsilon_{ij} = \tfrac{1}{2}(u_{i,j} + u_{j,i}), \tag{1c}$$

where σ_{ij} and ε_{ij} are the stress and strain tensors, respectively; C_{ijkl} is the elastic modulus tensor in classical isotropic elasticity; and u_i is the displacement vector. $\alpha(|x-x'|,\tau)$ is the nonlocal modulus or attenuation function, which incorporates the nonlocal effects at the reference point x that are produced by local strain at the source x' into the constitutive equations. $|x-x'|$ is the Euclidean distance. In $\tau = e_0 a/l$, e_0 is a constant appropriate to each material, a is an internal characteristic length (e.g., the length of the C–C bond, lattice parameter, granular distance), and l is an external characteristic length (e.g., crack length, wavelength).

The integral–partial differential equations of linear nonlocal elasticity are reduced to singular partial differential equations of a special class of physically admissible kernel (Eringen, 1983). Thus, Hook's law for the stress and strain relation in the polar coordinate system is expressed by

$$\sigma_x - (e_0 a)^2 \nabla^2 \sigma_x = \frac{E}{1-\upsilon^2}(\varepsilon_x + \upsilon \varepsilon_\theta), \tag{2a}$$

$$\sigma_\theta - (e_0 a)^2 \nabla^2 \sigma_\theta = \frac{E}{1-\upsilon^2}(\varepsilon_\theta + \upsilon \varepsilon_x), \tag{2b}$$

$$\sigma_{\theta x} - (e_0 a)^2 \nabla^2 \sigma_{\theta x} = \frac{E}{2(1+\upsilon)}\gamma_{x\theta}, \tag{2c}$$

$$\sigma_{x\theta} - (e_0 a)^2 \nabla^2 \sigma_{x\theta} = \frac{E}{2(1+\upsilon)}\gamma_{x\theta} a, \tag{2d}$$

where E is the Young's modulus of the material, υ is the Poisson's ratio, x and θ are the longitudinal and angular circumferential coordinates, σ_x, σ_θ, $\sigma_{\theta x}$, and $\sigma_{x\theta}$ are the normal and shear stresses, and ε_x, ε_θ, and $\gamma_{x\theta}$ are the normal and shear strains. The Laplace operator in the polar coordinate system is given by $\nabla^2 = (\partial^2/\partial x^2)+(\partial^2/r^2\partial\theta^2)$, and r is the radius measured from the mid-plane of the cross-section in the following CNT analysis. The parameter $e_0 a$ is the scale coefficient revealing the small-scale effect on the responses of structures of nano-size. The parameter $e_0 = 0.39$ was given by Eringen (1983). But there are no experiments conducted to determine the value of e_0 for CNT. Wang and Hu (2005) proposed $e_0 = 1/\sqrt{12} \approx 0.288$ used in the nonlocal beam model. Zhang et al. (2005) estimated $e_0 \approx 0.82$ by matching the theoretical buckling strain obtained by the nonlocal thin shell model (Zhang et al., 2004) to those from molecular mechanics simulations given by Sears and Batra (2004). A conservative estimate of the scale coefficient $e_0 a < 2.0$ nm for a SWCNT if the measured wave propagation frequency value for the SWCNT is greater than 10 THz (Wang, 2005). In this study, we will fix $a = 0.142$ nm and give the estimation of parameter e_0 by matching the dispersions of CNTs observed from the MD results with the numerical results obtained from the nonlocal shell model. The parameter a will be assumed to be independent of the length, diameter, and chirality of CNTs for the wave dispersion.

The nonlocal elastic cylindrical shell theory, which is based on the Flugge shell theory (Flugge, 1960), was developed by Wang and Varadan (2007). The application of the nonlocal elastic cylindrical shell theory to each tube of an armchair–armchair (10,10)@(15,15) DWCNT yields six equations that govern its free vibrations, as follows:

$$r_k^2\frac{\partial^2 u_k}{\partial x^2} + \frac{1}{2}(1-\upsilon)\frac{\partial^2 u_k}{\partial \theta^2} + \frac{r_k}{2}(1+\upsilon)\frac{\partial^2 v_k}{\partial x \partial \theta} - \upsilon r_k \frac{\partial w_k}{\partial x} + (1-\upsilon^2)\frac{D}{Ehr_k^2}\left(\frac{1}{2}(1-\upsilon)\frac{\partial^2 u_k}{\partial \theta^2} + r_k^3\frac{\partial^3 w_k}{\partial x^3} - \frac{r_k}{2}(1-\upsilon)\frac{\partial^3 w_k}{\partial x \partial \theta^2}\right)$$
$$= \frac{\rho h}{Eh}(1-\upsilon^2) r_k^2 (1-(e_0 a)^2\nabla^2)\frac{\partial^2 u_k}{\partial t^2}, \tag{3a}$$

$$\frac{r_k}{2}(1+\upsilon)\frac{\partial^2 u_k}{\partial x \partial \theta} + \frac{r_k^2}{2}(1-\upsilon)\frac{\partial^2 v_k}{\partial x^2} + \frac{\partial^2 v_k}{\partial \theta^2} - \frac{\partial w_k}{\partial \theta} + (1-\upsilon^2)\frac{D}{Eh}\left(\frac{3}{2}(1-\upsilon)\frac{\partial^2 v_k}{\partial x^2} + \frac{1}{2}(3-\upsilon)\frac{\partial^3 w_k}{\partial x^2 \partial \theta}\right)$$
$$= \frac{\rho h}{Eh}(1-\upsilon^2) r_k^2 (1-(e_0 a)^2\nabla^2)\frac{\partial^2 v_k}{\partial t^2}, \tag{3b}$$

$$\upsilon r_k \frac{\partial u_k}{\partial x} + \frac{\partial v_k}{\partial \theta} - w_k - (1-\upsilon^2)\frac{D}{Ehr_k^2}\left(r_k^4\nabla^2\nabla^2 w_k + r_k^3\frac{\partial^3 u_k}{\partial x^3} - \frac{r_k}{2}(1-\upsilon)\frac{\partial^3 u_k}{\partial x \partial \theta^2} + \frac{r_k^2}{2}(3-\upsilon)\frac{\partial^3 v_k}{\partial x^2 \partial \theta} + w_k + 2\frac{\partial^2 w_k}{\partial \theta^2}\right)$$
$$= \frac{1}{Eh}(1-\upsilon^2) r_k^2 (1-(e_0 a)^2\nabla^2)\left(\frac{\partial^2 w_k}{\partial t^2}\rho h - p_k\right), \tag{3c}$$

where p_k $(k = 1,2)$ is the van der Waals (vdW) force between the adjacent tubes. The (inward positive) net radial pressure p_k on tube k is given as follows:

$$p_1 = c_{12}(\omega_1 - \omega_2) \quad \text{and} \quad p_2 = c_{21}(\omega_2 - \omega_1), \tag{4}$$

where c_{ij} $(i,j = 1,2)$ is the vdW interaction coefficient, which is estimated as (He et al., 2005)

$$c_{ij} = -\left[\frac{1001\pi\varepsilon\sigma^{12}}{3a^4}E_{ij}^{13} - \frac{1120\pi\varepsilon\sigma^6}{9a^4}E_{ij}^{7}\right]R_j, \tag{5}$$

where

$$E_{ij}^{m} = (R_j + R_i)^{-m} \int_0^{\pi/2} \frac{\mathrm{d}\theta}{[1 - K_{ij}\cos^2\theta]^{m/2}} \tag{6}$$

and

$$K_{ij} = \frac{4R_jR_i}{(R_j + R_i)^2}. \tag{7}$$

The wave propagation solution for CNTs can be expressed as

$$u(x,t) = U\mathrm{e}^{\mathrm{i}(lx+m\theta-\omega t)}, \tag{8a}$$

$$v(x,t) = V\mathrm{e}^{\mathrm{i}(lx+m\theta-\omega t)}, \tag{8b}$$

$$w(x,t) = W\mathrm{e}^{\mathrm{i}(lx+m\theta-\omega t)}, \tag{8c}$$

where U, V, and W denote the longitudinal, circumferential, and radial displacement amplitudes of tube k, respectively. l is the wavenumber in the longitudinal direction, ω is the frequency of the wave motion. The proposed nonlocal Flugge shell theory in Eqs. (3a)–(3c) can conform to the local theory if the scale coefficient, $e_0a = 0$, is set to zero.

An important case result from considering motion independent of θ. Thus $\partial/\partial\theta = 0$

$$r^2\frac{\partial^2 u}{\partial x^2} - \upsilon r\frac{\partial w}{\partial x} + (1-\upsilon^2)\frac{D}{Ehr^2}r^3\frac{\partial^3 w}{\partial x^3} = \frac{\rho h}{Eh}(1-\upsilon^2)r^2(1-(e_0a)^2\nabla^2)\frac{\partial^2 u}{\partial t^2} \tag{9a}$$

$$\frac{r^2}{2}(1-\upsilon)\frac{\partial^2 v}{\partial x^2} + (1-\upsilon^2)\frac{D}{Eh}\frac{3}{2}(1-\upsilon)\frac{\partial^2 v}{\partial x^2} = \frac{\rho h}{Eh}(1-\upsilon^2)r^2(1-(e_0a)^2\nabla^2)\frac{\partial^2 v}{\partial t^2}, \tag{9b}$$

$$\upsilon r\frac{\partial u}{\partial x} - w - (1-\upsilon^2)\frac{D}{Ehr^2}\left(r^4\nabla^2\nabla^2 w + r^3\frac{\partial^3 u}{\partial x^3}\right) = \frac{1}{Eh}(1-\upsilon^2)r^2(1-(e_0a)^2\nabla^2)\left(\frac{\partial^2 w}{\partial t^2}\rho h - p\right). \tag{9c}$$

Eq. (9b) is uncoupled from the other two equations and represents the purely torsional motion of the shell. The pure torsional wave propagation solution for CNTs can be expressed as $v(x,t) = V\mathrm{e}^{\mathrm{i}}(kx-\omega t)$. Substituting the expression to Eq. (9b) leads to the velocity of torsion wave:

$$v = \frac{1}{1-(e_0a)^2k^2}\left(\frac{E}{2\rho(1+\upsilon)} + \frac{3D(1-\upsilon)}{2h\rho r^2}\right). \tag{10}$$

The material parameters of CNTs are proposed as: in-plane stiffness $Eh = 360\,\mathrm{J/m^2}$ (Yakobson et al., 1996), mass density $\rho h = (2.27\,\mathrm{g/cm^3}) \times 0.34\,\mathrm{nm}$.

Adams et al. (1992) suggested the bending rigidity, $D = 1.62\,\mathrm{eV}$, by applying the quantum MD methods using both empirical and local density functional methods to evaluate the energies of a number of ball-shaped and tubular fullerenes of various sizes. The bending rigidity $D = 1.46\,\mathrm{eV}$ was evaluated based on *ab initio* energy calculations by Kudin et al., (2001). The value of bending rigidity, $D = 2\,\mathrm{eV}$, was proposed in a study in which the results of the phonon dispersion relations of a CNT were compared with those based on the local elasticity theory for a cylindrical medium (Wang et al., 2005). Wang and Liew (2008) proposed the bending rigidity 1.78 eV using molecular mechanics calculations for relatively large tubes and graphite sheets. $D = 1.78\,\mathrm{eV}$ will be used in this study. The substitution of Eqs. (9a)–(9c) into Eqs. (3a)–(3c) ultimately yields a generalized eigenvalue problem, as follows:

$$M\{(l,m),\omega\}_{6\times 6}\begin{Bmatrix} U_1 \\ V_1 \\ W_1 \\ U_2 \\ V_2 \\ W_2 \end{Bmatrix} = 0, \tag{11}$$

where the entries of matrices M are functions of the wavenumbers l and ω and the scale coefficient e_0a. The condition for the existence of nonzero solutions U_k and W_k $(k = 1, 2)$ is

$$\det M = 0. \tag{12}$$

The six dispersion relations can be obtained by solving Eq. (12) for a given wavenumber $m = 2$. The numerical results are shown in Fig. 1. One of them will be used to predict the dispersion of the transverse wave in an armchair–armchair (10,10)@(15,15) DWCNT.

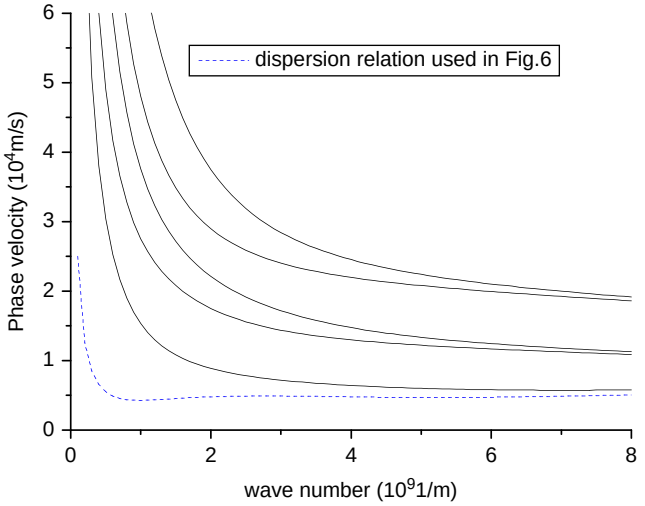

Fig. 1. Wave velocity versus wavenumber of the armchair–armchair (10,10)@(15,15) DWCNT at wavenumber $m = 2$.

3. Molecular dynamics model for carbon nanotubes

To check the applicability of the dispersion relations produced by the nonlocal cylindrical shell model to SWCNTs and DWCNTs, MD simulations are presented. The transverse and torsional wave can be produced when the atoms at the end of CNT are excited in a way showed in Fig. 1(a) and (b), respectively. The lengths of SWCNTs and DWCNTs are about 19.7 nm.

In the corresponding MD models, the interaction of the atoms in each tube is described by the second-generation REBO potential energy expression for hydrocarbons, whereas the van der Waals force between the inner and outer walls is described by the Lennard-Jones (1924) potential. In the second-generation REBO potential, the total potential energy of the system is given by

$$E_{\mathrm{REBO}} = \sum_i \sum_{j=i+1} [E_{\mathrm{R}}(r_{ij}) - \overline{b}_{ij} E_{\mathrm{A}}(r_{ij})], \tag{13}$$

where r_{ij} is the distance between the pairs of adjacent atoms i and j, and b_{ij} is a many-bond empirical bond-order term between the atoms i and j that is derived from the Huckel electronic structure theory. E_{R} and E_{A} are the repulsive and attractive pair terms, respectively:

$$E_{\mathrm{R}}(r) = f_{\mathrm{c}}(r)\left(1 + \frac{Q}{r}\right) A \exp(-\alpha r), \tag{14}$$

$$E_{\mathrm{A}}(r) = f_{\mathrm{c}}(r) \sum_{n=1}^{3} B_n \mathrm{e}^{-\beta_n r}, \tag{15}$$

where the parameters Q, A, α, B, β are used to fit the pair terms, and the values for all parameters are given by Brenner et al (2002). The function f_{c} is a cutoff function and is given by

$$f_{\mathrm{c}}(r) = \begin{cases} 1, & r < R_{\min}, \\ \{1+\} \cos\left[\dfrac{\pi(r - R_{\min})}{(R_{\max} - R_{\min})}\right] \Big/ 2, & R_{\min} < r < R_{\max}, \\ 0, & r > R_{\max}, \end{cases} \tag{16}$$

where $R_{\max} - R_{\min}$ defines the distance over the function that goes from one to zero. For graphite and CNTs, $R_{\max} = 0.2$ nm and $R_{\min} = 0.17$ nm, respectively.

The van der Waals interaction between the inner and outer walls is modeled by the Lennard-Jones potential, as follows:

$$V_{ij}(r_{ij}) = 4\xi \left[\left(\frac{\sigma}{r_{ij}}\right)^{12} - \left(\frac{\sigma}{r_{ij}}\right)^{6} \right], \tag{17}$$

where the coefficients of well-depth energy ξ and the equilibrium distance σ are 4.20383×10^{-3} eV and 3.4 Å, respectively (Moller et al., 1991).Using the second-generation REBO potential, we computed the Poisson's ratio $v = 0.317$ and Young's modulus $E = 0.83$ TPa for the armchair (10,10) and (15,15) CNTs that were derived from the MD simulation for the test of axial tension. The Poisson's ratio $v = 0.347$ and Young's modulus $E = 0.8$ TPa are calculated for the zigzag (20,0) CNT.

4. Results and discussion

It is quite straightforward to determine the phase velocity and wavenumber from the transverse vibration of atoms in two arbitrary sections of a CNT that was simulated using MD. The harmonic deflection of some atoms was achieved by shifting the atoms at one end of the nanotube while the other end was kept free as showed in Fig. 2(a). For example, some atoms that are located at the end of the armchair (15,15) SWCNT denoted by Section 0 were assumed to be subject to the harmonic deflection of period $T = 500$ fs, as shown in Fig. 3(a). The corresponding angular frequency is $\omega = 2\pi/T \approx 1.26 \times 10^{13}$ rad/s. Figs. 3(b) and (c) show the transverse vibrations of the atom in Section 1 at $x_1 = 2.46$ nm and Section 2 at $x_2 = 4.92$ nm, respectively. If the transient deflection of the first two periods is neglected, then the propagation duration Δt of the wave from Section 1 to Section 2 can be estimated as

$$\Delta t \approx \frac{(t_{23} - t_{13}) + (t_{24} - t_{14}) + \cdots + (t_{2n} - t_{1n})}{n - 2}. \tag{18}$$

The phase velocity and wavenumber are, respectively

$$c = \frac{x_2 - x_1}{\Delta t}, \quad k = \frac{2\pi}{\lambda} = \frac{\omega T}{\lambda} = \frac{\omega}{c}. \tag{19}$$

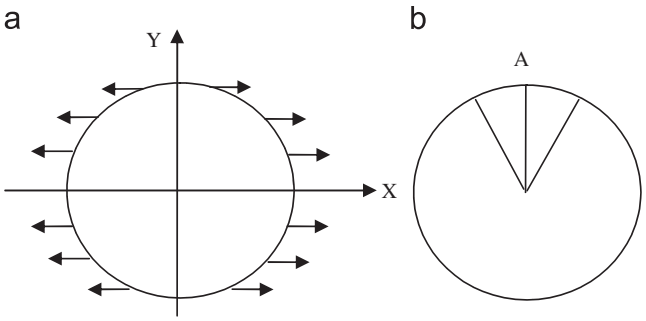

Fig. 2. (a) The atoms at the end of the CNT are subjected to harmonic excitation to move in different direction at the same time and (b) every atom like atom A at the end of the CNT swings through a small angle after exited.

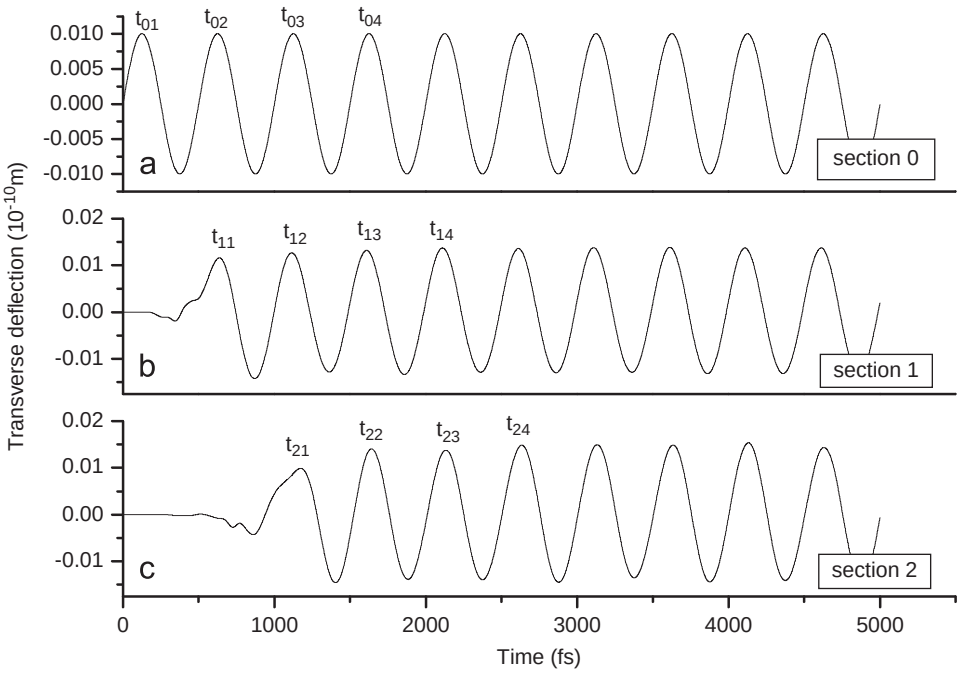

Fig. 3. Time histories of the deflection of atom at different sections of the armchair (15,15) CNT: (a) the sinusoidal wave of period $T = 500$ fs input at Section 0, (b) the deflection of Section 1, 2.46 nm ahead of Section 0, and (c) the deflection of Section 2, 4.92 nm ahead of Section 0.

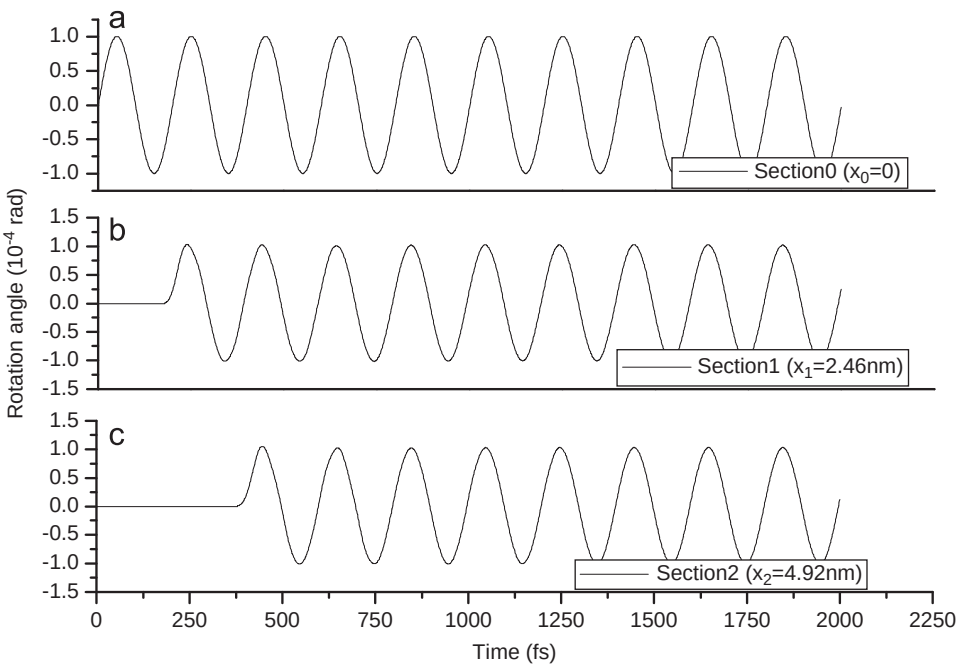

Fig. 4. The time histories of the rotation angle of different sections of the armchair (10,10) SWCNT: (a) the sinusoidal wave of period $T = 200$ fs input at Section 0, (b) the deflection of Section 1, 2.46 nm ahead of Section 0, and (c) the deflection of Section 2, 4.92 nm ahead of Section 0.

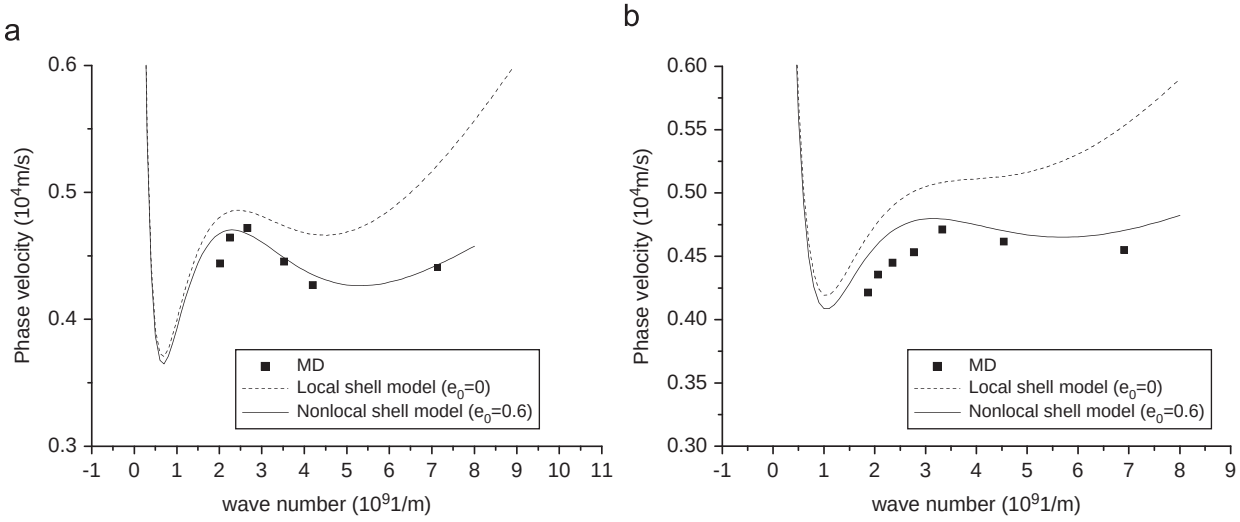

Fig. 5. Dispersion relation of transverse wave in the (a) armchair (15,15) carbon nanotube and (b) zigzag (20,0) carbon nanotube.

When the atoms at the end of CNT are subjected to the harmonic excitation indicated in Fig. 2(b), the torsional wave will propagate in SWCNT showed in Fig. 4. The torsional wave velocity can be calculated through the method for calculating transverse wave velocity.

Figs. 5 illustrates the dispersion relations between the phase velocity c and the wavenumber k of the transverse wave in the armchair (15,15) SWCNT and zigzag (20,0) SWCNT. Figs. 5 shows the nonlocal shell model can predict the MD results better than the local shell model can when the wavelengths are less than 2.36×10^{-9} and 1.88×10^{-9} m for (15,15) SWCNT and (20,0) SWCNT, respectively. The value of the parameter $e_0 = 0.6$ is used for transverse wave in armchair (15,15) and zigzag (20,0) CNT.

Fig. 6 shows that the nonlocal elastic cylindrical double-shell model can predict the dispersion relation of the transverse wave better than local double-shell model when the wavenumber is large enough. This is because the interlayer van der Waals interaction of the DWCNT and the small-scale effect on the dispersion of the transverse wave of

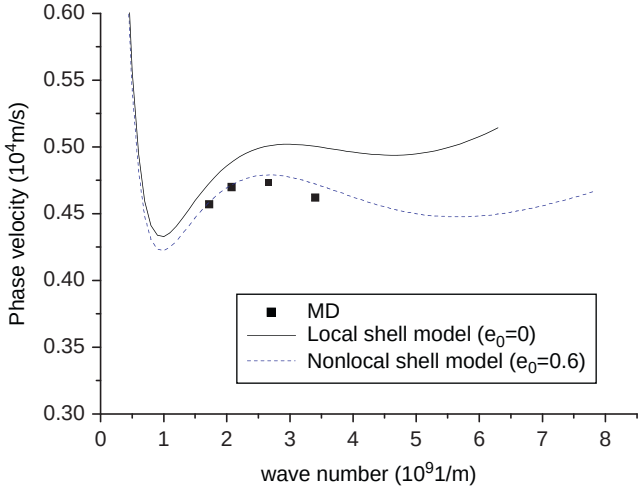

Fig. 6. Dispersion relation of the armchair–armchair (10,10)@(15,15) DWCNT.

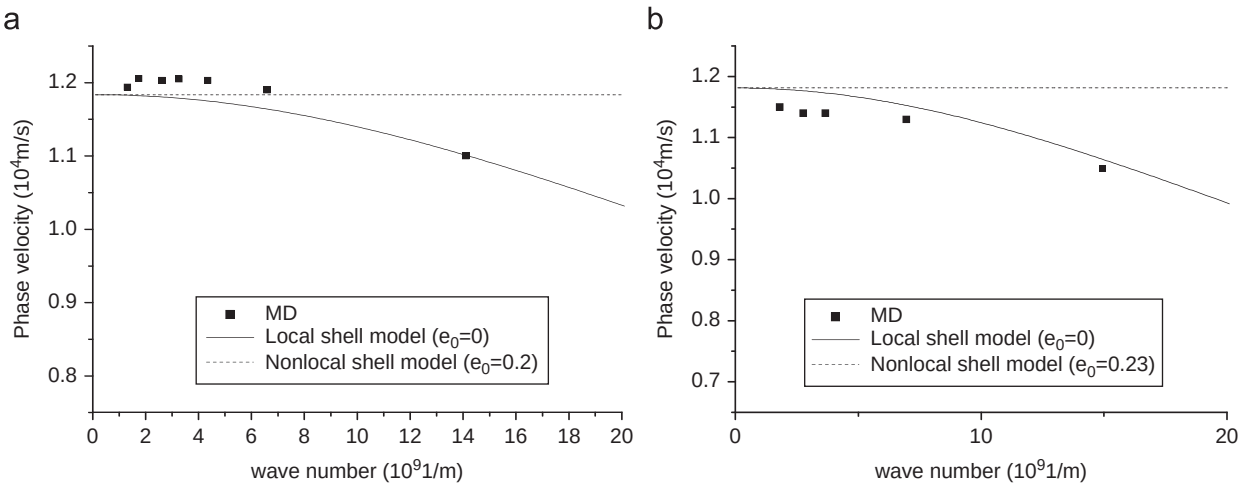

Fig. 7. Dispersion relation of torsional wave in the armchair (a) (10,10) and (b) (15,15) SWCNT.

the SWCNT are considered. The phase velocity decreases when the wavenumber is approximately larger than 2.65×10^9 l/m, or the wavelength is approximately less than 2.35×10^{-9} m. The nonlocal elastic double-shell model can predict the wave dispersion better than local shell model when the wavelength is approximately smaller than 2.35×10^{-9} m. Fig. 7 indicates that the nonlocal shell model can predict dispersion relation obtained from the MD simulation of torsional wave in (10,10) SWCNT and (15,15) SWCNT better than local shell model can when the wavelength is smaller than 0.95×10^{-9} and 0.9×10^{-9} m, respectively. The good agreement between the nonlocal elastic cylindrical shell models results and the MD simulations verifies the effectiveness of this model. The value of the parameter $e_0=0.6$ is adopted for (10,10)@(15,15) DWCNT to predict the dispersion of transverse wave in CNTs, and $e_0=0.2$ and 0.23 are used for torsional wave in SWCNT (10,10) and SWCNT (15,15), respectively. The estimates of e_0 are investigated through the comparison between the dispersion relations obtained from numerical results of equations and MD simulation. The value of e_0 which is a coefficient to identify the scale effect should be different for different issues, such as dispersions of different elastic waves in SWCNT and DWCNT. The scale coefficient is dependent on SWCNT and DWCNT for transverse wave, and CNTs for torsional wave. When the vale of e_0 becomes smaller, the scale effect will be weaker. The torsional wave motion is only related to the displacement in tangential direction, while the transverse wave motion is involved in the displacements in longitudinal, radial, and tangential direction. The carbon atoms vibrating more complicated in the transverse wave propagation in CNT leads to the stronger scale effect on the dispersion of transverse wave. This is the main reason why the vale of $e_0=0.2$ for the torsional wave in SWCNT is much smaller than the values of $e_0=0.6$ used for transverse wave in CNTs. The structure of CNTs, such as chirality, diameter and layers, may also be the factors to affect the value of e_0. But for the same problem such as transverse wave or torsional wave in CNT, these

structure differences lead to relative small change of the value of e_0 compared to the changes of values for different problems.

Fig. 8 indicates that the obvious phase difference of inner and outer tube of the (10,10)@(15,15) DWCNT will occur at the period $T = 300$ fs. The corresponding angular frequency is $\omega = 2\pi/T \approx 3.14 \times 10^{13}$ rad/s. The average phase difference between the inner tube and the outer tube can be estimated from Fig. 8 as $\bar{t} = (1/n)\sum_{i=1}^{n}(t_{0i} - t_{1i}) \approx 103.2$ fs. Fig. 9 indicates that the SWCNTs (10,10) and (15,15) have different phases at the period $T = 300$ fs without considering the van der Waals forces between them. The average phase difference between the SWCNTs (10,10) and (15,15) can also be estimated

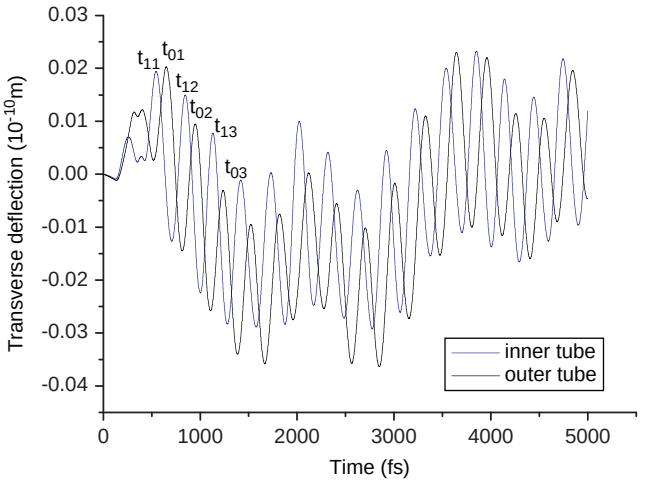

Fig. 8. The time histories of the deflection of atom at the section, 2.46 nm ahead of the end of the armchair–armchair (10,10)@(15,15) DWCNT. The sinusoidal wave of period $T = 300$ fs input at the end of the DWCNT.

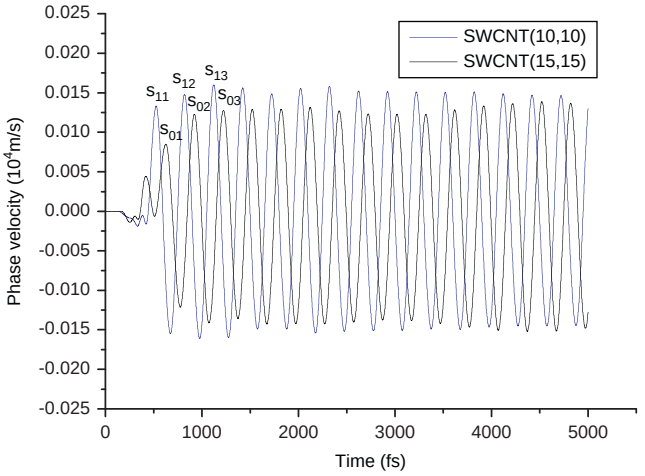

Fig. 9. The time histories of the deflection of atom at the section, 2.46 nm ahead of the end of the SWCNT (10,10) and SWCNT (15,15). The sinusoidal wave of period $T = 300$ fs input at the end of the SWCNTs.

Table 1
The average phase differences of the vibrations of atom at the section, 2.46 nm ahead of the end of the DWCNTs (10,10)@(15,15) and the SWCNTs (10,10) and (15,15)

Period (fs)	DWCNTs (10,10)@(15,15) (fs)	SWCNTs (10,10) and (15,15) (fs)	$\lvert\bar{s} - \bar{t}\rvert$ (fs)
$T = 300$	$\bar{t} = 103.2$	$\bar{s} = 101.2$	2
$T = 400$	$\bar{t} = 80.3$	$\bar{s} = 74.1$	6.2
$T = 500$	$\bar{t} = 59.8$	$\bar{s} = 38.8$	21
$T = 600$	$\bar{t} = 54$	$\bar{s} = 29$	25
$T = 700$	$\bar{t} = 43.3$	$\bar{s} = 40$	3.3

from Fig. 9: $\bar{s} = (1/n)\sum_{i=1}^{n}(s_{0i} - s_{1i}) \approx 101.2$ fs. The other average phase differences at different periods are shown in Table 1. The phase difference of the vibration becomes increasingly obvious with the decrease of the period. The phase difference increases from 43.3 to 103.2 fs as the period decreases from 700 to 300 fs for DWCNTs. Similarly, the phase difference increases from 40 to 101.2 fs as the period decreases from 700 to 300 fs for SWCNTs. The van der Waals forces make no significant contribution to the phase differences of the transverse wave in the inner and outer tube, as the phase differences would occur without consideration of the van der Waals forces between the adjacent tubes. This indicates that the small-scale effects can change the phase when the frequency is extremely high.

5. Concluding remarks

This paper presents a study of transverse and torsional wave dispersion in SWCNT and DWCNTs on the basis of the nonlocal elastic cylindrical shell theory and the use of MD simulations for SWCNT and an armchair–armchair (10,10)@(15,15) DWCNT in a wide range of wavenumbers. The value of parameter e_0 is estimated based on the MD result to predict the dispersion of transverse wave in CNTs through using the nonlocal shell models. The results of this study indicate that the nonlocal elastic cylindrical shell model is able to offer a better prediction for transverse and torsional wave dispersion in CNTs than the local elastic shell model when the wavenumber is large enough. The nonlocal shell models are required when the wavelengths are approximately less than 2.36×10^{-9} and 0.95×10^{-9} m for transverse wave in armchair (15,15) SWCNT and torsional wave in armchair (10,10) SWCNT, respectively. These small-scale effects have a significant effect on the phase difference of transverse wave in inner and outer tube of DWCNTs at high frequency.

Acknowledgements

The work described in this paper was fully supported by the City University of Hong Kong Strategic Research Grant Project no. 7002204 and a Canada Research Chair Program. The work was also supported by the computing facilities provided by the ACIM.

References

Adams, G.B., Sankey, O.F., Page, J.B., Okeeffe, M., Drabold, D.A., 1992. Energetics of large fullerenes—balls, tubes, and capsules. Science 256 (5065), 1792–1795.
Ball, P., 2001. Roll up for the revolution. Nature 414, 142–144.
Baughman, R.H., Zakhidov, A.A., de Heer, W.A., 2002. Carbon nanotubes—the route toward applications. Science 297, 787–792.
Brenner, D.W., 1990. Empirical potential for hydrocarbons for use in simulating the chemical vapor-deposition of diamond films. Phys. Rev. B 42, 9458.
Brenner, D.W., Shenderova, O.A., Harrison, J.A., Stuart, S.J., Ni, B., Sinnott, S.B., 2002. A second-generation reactive empirical bond order (REBO) potential energy expression for hydrocarbons. J. Phys.: Condens. Matter 14, 783–802.
Eringen, A.C., 1976. Nonlocal Polar Field Models. Academic, New York.
Eringen, A.C., 1983. On differential equations of nonlocal elasticity and solutions of screw dislocation and surface waves. J. Appl. Phys. 54, 4703.
Flugge, W., 1960. Stresses in Shells. Springer, Berlin/Heidelberg.
Govindjee, S., Sackman, J.L., 1999. On the use of continuum mechanics to estimate the properties of nanotubes. Solid State Commun. 110, 227.
He, X.Q., Kitipornchai, S., Liew, K.M., 2005. Buckling analysis of multi-walled carbon nanotubes: a continuum model accounting for van der Waals interaction. J. Mech. Phys. Solids 53 (2), 303–326.
Hernandez, E., Goze, C., Bernier, P., Rubio, A., 1998. Elastic properties of C and $B_xC_yN_z$ composite nanotubes. Phys. Rev. Lett. 80, 4502.
Iijima, S., 1991. Helical microtubes of graphitic carbon. Nature 354, 56–58.
Iijima, S., Brabec, C., Maiti, A., Bernholc, J., 1996. Structural flexibility of carbon nanotubes. Chem. Phys. 104, 2089.
Insepov, Z., Wolf, D., Hassanein, A., 2006. Nanopumping using carbon nanotubes. Nano Lett 6 (9), 1893–1895.
Krishnan, A., Dujardin, E., Ebbesen, T.W., Yianilos, P.N., Treacy, M.M.J., 1998. Young's modulus of singled-walled nanotubes. Phys. Rev. B 58, 14013–14019.
Kudin, K.N., Scuseria, G.E., Yakobson, B.I., 2001. C_2F, BN, and C nanoshell elasticity from ab initio computations. Phys. Rev. B 64, 235406.
Lau, K.T., 2003. Interfacial bonding characteristics of nanotube/polymer composites. Chem. Phys. Lett. 370, 399–405.
Lennard-Jones, J.E., 1924. The determination of molecular fields: from the variation of the viscosity of a gas with temperature. Proc. R. Soc. 106A, 441.
Li, C.Y., Chou, T.W., 2006. Elastic wave velocities in single-walled carbon nanotubes. Phys. Rev. B 73, 245407.
Liew, K.M., Wang, Q., 2007. Analysis of wave propagation in carbon nanotubes via elastic shell theories. Int. J. Eng. Sci. 45, 227–241.
Liew, K.M., He, X.Q., Wong, C.H., 2004a. On the study of elastic and plastic properties of multi-walled carbon nanotubes under axial tension using molecular dynamics simulation. Acta Mater. 52, 2521–2527.
Liew, K.M., Wong, C.H., He, X.Q., Tan, M.J., Meguid, S.A., 2004b. Nanomechanics of single and multi-walled carbon nanotubes. Phys. Rev. B 69, 115429.
Liew, K.M., Wong, C.H., Tan, M.J., 2006. Tensile and compressive properties of carbon nanotube bundles. Acta Mater. 54, 225–231.
Liew, K.M., Hu, Y.G., He, X.Q., 2008. Transverse wave propagation in single-walled carbon nanotubes. J. Comput. Theor. Nanosci. 5 (4), 581–586.
Lourie, Q., Cox, D.M., Wagner, H.D., 1998. Buckling and collapse of embedded carbon nanotubes. Phys. Rev. Lett. 81, 1638–1641.
Moller, M.A., Tildesley, D.J., Kim, K.S., Quirke, N., 1991. Molecular dynamics simulation of a Langmuir–Blodgett film. J. Chem. Phys. 94, 8390–8401.
Natsuki, T., Endo, M., Tsuda, H., 2006. Vibration analysis of embedded carbon nanotubes using wave propagation approach. J. Appl. Phys. 99, 034311.
Natsuki, T., Ni, Q.Q., Endo, M., 2007. Wave propagation in single- and double-walled carbon nanotubes filled with fluids. J. Appl. Phys. 101, 034319.
Parnes, R., Chiskis, A., 2002. Buckling of nano-fiber reinforced composites: a re-examination of elastic buckling. J. Mech. Phys. Solids 50, 855–879.
Peddieson, J., Buchanan, G.R., McNitt, R.P., 2003. Application of nonlocal continuum models to nanotechnology. Int. J. Eng. Sci. 41, 305–312.
Ru, C.Q., 2000a. Effective bending stiffness of carbon nanotubes. Phys. Rev. B 62, 9973–9976.
Ru, C.Q., 2000b. Elastic buckling of single-walled carbon nanotube ropes under high pressure. Phys. Rev. B 62, 10405–10408.
Sanchez-Portal, D., Artacho, E., Soler, J.M., Rubio, A., Ordejon, P., 1999. Ab initio structural, elastic, and vibrational properties of carbon nanotubes. Phys. Rev. B 59, 12678–12688.
Sears, A., Batra, R.C., 2004. Macroscopic properties of carbon nanotubes from molecular–mechanics simulations. Phys. Rev. B 69, 235406.
Sharma, P., Ganti, S., Bhate, N., 2003. Effect of surfaces on the size-dependent elastic state of nano-inhomogeneities. Appl. Phys. Lett. 82, 535–537.
Sheehan, P.E., Lieber, C.M., 1996. Nanotribology and nanofabrication of MoO_3 structures by atomic force microscopy. Science 272, 1158–1161.

Sudak, L.J., 2003. Column buckling of multiwalled carbon nanotubes using nonlocal continuum mechanics. J. Appl. Phys. 94 (11), 7281.
Sun, C.T., Zhang, H., 2003. Size-dependent elastic moduli of platelike nanomaterials. J. Appl. Phys. 93, 1212–1218.
Wang, C.Y., Ru, C.Q., Mioduchowski, A., 2005. Axisymmetric and beamlike vibrations of multiwall carbon nanotubes. Phys. Rev. B 72, 075414.
Wang, L.F., Hu, H.Y., 2005. Transverse wave propagation in single-walled carbon nanotubes. Phys. Rev. B 71, 195412.
Wang, Q., 2004. Effective in-plane stiffness and bending rigidity of armchair and zigzag carbon nanotubes. Int. J. Solids Struct. 41, 5451–5461.
Wang, Q., 2005. Wave propagation in carbon nanotubes via nonlocal continuum mechanics. J. Appl. Phys. 98, 124301.
Wang, Q., Varadan, V.K., 2007. Application of nonlocal elastic shell theory in wave propagation analysis of carbon nanotubes. Smart Mater. Struct. 16, 178–190.
Wang, Q., Liew, K.M., 2008. Molecular mechanics modeling for properties of carbon nanotubes. J. Appl. Phys. 103 (4), 046103.
Wong, E.W., Sheehan, P.E., Lieber, C.M., 1997. Nanobeam mechanics: elasticity, strength, and toughness of nanorods and nanotubes. Science 277, 1971–1975.
Yakobson, B.I., Brabec, C.J., Bernholc, J., 1996. Nanomechanics of carbon tubes: instabilities beyond linear response. Phys. Rev. Lett. 76, 2511–2514.
Yakobson, B.I., Campbell, M.P., Brabec, C.J., Bernholc, J., 1997. High strain rate fracture and C-chain unraveling in carbon nanotubes. Comput. Mater. Sci. 8, 341–348.
Zhang, Y.Q., Liu, G.R., Wang, J.S., 2004. Small-scale effects on buckling of multiwalled carbon nanotubes under axial compression. Phys. Rev. B 70, 205430.
Zhang, Y.Q., Liu, G.R., Xie, X.Y., 2005. Free transverse vibration of double-walled carbon nanotubes using a theory of nonlocal elasticity. Phys. Rev. B 71, 195404.